RESEARCH ARTICLE

Arp2/3 nucleates F-actin coating of fusing insulin granules in pancreatic β cells to control insulin secretion

Wei Ma[1], Jenny Chang[2], Jason Tong[1], Uda Ho[2], Belinda Yau[1], Melkam A. Kebede[1] and Peter Thorn[1],*

ABSTRACT

F-actin dynamics are known to control insulin secretion, but the point of intersection with the stimulus-secretion cascade is unknown. Here, using multiphoton imaging of β cells isolated from Lifeact-GFP transgenic mice, we show that glucose stimulation does not cause global changes in subcortical F-actin. Instead, we observe spatially discrete and transient F-actin changes around each fusing granule. This F-actin remodelling is dependent on actin nucleation and is observed for granule fusion induced by either glucose or high potassium stimulation. Using GFP-labelled proteins, we identify local enrichment of Arp3, dynamin 2 and clathrin, all occurring after granule fusion, suggesting early recruitment of an endocytic complex to the fusing granules. Block of Arp2/3 activity with drugs or shRNA inhibits F-actin coating, traps granules at the cell membrane and reduces insulin secretion. Block of formin-mediated actin nucleation also blocks F-actin coating, but has no effect on insulin secretion. We conclude that local Arp2/3-dependent actin nucleation at the sites of granule fusion plays an important role in post-fusion granule dynamics and in the regulation of insulin secretion.

KEY WORDS: Actin, β cells, Exocytosis, Insulin

INTRODUCTION

Regulated secretion is defined by a series of steps that link cell stimulation to secretory granule fusion and the release of granule content (Anantharam and Kreutzberger, 2019). In pancreatic β cells, this cascade links glucose stimulation to the secretion of insulin (Ashcroft and Rorsman, 2012). It has long been recognised that F-actin plays a key role in the control of insulin secretion (Orci et al., 1972; Mourad et al., 2010), with more recent mechanistic insights (Tomas et al., 2006; Wang et al., 2007; Uenishi et al., 2013). However, the actual point(s) at which F-actin exerts its influence in the secretory cascade controlling insulin secretion is unknown.

One important potential step is the interaction of secretory granules with the subcortical actin cytoskeleton (Li et al., 2018). In support of this, there is a large body of data demonstrating that manipulating the F-actin cytoskeleton has dramatic effects on secretion (Muallem et al., 1995; Mourad et al., 2010; Orci et al., 1972), and imaging studies show that changes in the F-actin structure can be linked with the movement of the granule

towards the plasma membrane (Orci et al., 1972; Heaslip et al., 2014) and subsequent granule behaviour after fusion (Valentijn et al., 2000).

However, because F-actin structures and dynamics are different for different secretory cell types, there is no consensus model describing the role of F-actin in granule fusion. For example, exocrine acinar cells confine regulated secretion to the apical region, which is marked by polarised enrichment of an extensive F-actin network (Valentijn et al., 1999; Nemoto et al., 2004; Turvey and Thorn, 2004). In contrast, although endocrine cells have recently been shown to be polarised (Gan et al., 2017), F-actin is distributed as a relatively homogeneous fine subcortical network (Orci et al., 1972; Gasman et al., 2004; Doreian et al., 2008). How these differences might affect the mechanisms and the role of F-actin in controlling secretion is not clear. Our understanding of these processes is hampered by the fact that F-actin plays many roles in the cell, including overall cell structure (Dominguez and Holmes, 2011) and membrane tension (Wen et al., 2016). Disrupting F-actin can therefore have many consequences on cell behaviour, and effects on secretion could be secondary to these. In addition, it is not possible using secretory assays to distinguish between any effects of F-actin remodelling before or after granule fusion (Uenishi et al., 2013; Wang et al., 2007).

This makes it necessary to image single-granule fusion events, which can be difficult for endocrine cells, which have small granules and relatively fast fusion events (Takahashi et al., 2002; Low et al., 2013). As a result, almost all work on F-actin remodelling during granule fusion has been performed on cell types with large (>1 μm) granules, such as oocytes (Yu and Bement, 2007; Sokac et al., 2003) and exocrine cells (Valentijn et al., 2000; Nemoto et al., 2004; Tran et al., 2015; Jang et al., 2012; Rousso et al., 2016). The prevailing view is that remodelling predominantly occurs after fusion and that F-actin coats each individual fusing granule (Tran et al., 2015; Nightingale et al., 2011; Turvey and Thorn, 2004; Nemoto et al., 2004). Granule fusion in these cell types is relatively slow (minutes), and, over time, as the granules collapse into the plasma membrane, the F-actin coat also shrinks (Sokac et al., 2003). There is some evidence that F-actin may be driving granule collapse through a contractile process (Miklavc et al., 2012; Sokac et al., 2003; Nightingale et al., 2011) and other evidence that F-actin controls the opening of the fusion pore (Larina et al., 2007; Ñeco et al., 2008; Doreian et al., 2008). If these findings were correct, this would place F-actin in a primary role in the control of secretion. Mechanistically, it is clear that F-actin remodelling after granule fusion occurs through actin nucleation (Tran et al., 2015; Gasman et al., 2004; Miklavc et al., 2012; Rousso et al., 2016). The branched chain nucleator Arp2/3 plays a role in many systems (Tran et al., 2015; Gasman et al., 2004; Rousso et al., 2016), and linear chain polymerisation is involved in some systems (Rousso et al., 2016; Miklavc et al., 2012; Wen et al., 2016). Upstream of these nucleators the control mechanisms include

[1]Discipline of Physiology, School of Medical Sciences, Charles Perkins Centre, University of Sydney, Camperdown 2006, Australia. [2]School of Biomedical Sciences, University of Queensland, St Lucia 4072, Australia.

*Author for correspondence (p.thorn@sydney.edu.au)

W.M., 0000-0002-8524-7605; J.T., 0000-0003-1027-3662; P.T., 0000-0002-3228-770X

1

WASP (Wen et al., 2016; Gasman et al., 2004; Tran et al., 2015) and Cdc42 (Sokac et al., 2003), with evidence that the primary trigger for actin nucleation is dependent on granule fusion (Sokac and Bement, 2006).

In endocrine cells with smaller granules (<0.5 µm), subcortical F-actin changes are observed to be coincident with granule fusion (Gasman et al., 2004). However, single-granule fusion studies in chromaffin cells showed inconsistent changes in F-actin (Wen et al., 2016). Whether this reflects a difference with the fusion of large granules or whether it is due to difficulties in imaging small granules is not clear. There are limited single-granule studies of the action of F-actin in pancreatic β cells (Heaslip et al., 2014), but there are reports that F-actin remodelling does occur during glucose stimulation and this does affect insulin secretion (Wang et al., 2007; Uenishi et al., 2013), as well as reported effects of actin-targeting drugs on secretion (Tomas et al., 2006; Orci et al., 1972). Where F-actin exerts its principal effects on the stimulus secretion pathway in β cells is therefore not clear.

Here, we set out to investigate the possible role of F-actin dynamics during insulin granule fusion in pancreatic β cells. We employed multiphoton imaging of single-granule fusion events and demonstrate that all events are associated with local, transient F-actin remodelling that coats individual granules. This coating is observed even with high-potassium stimulation, indicating that remodelling is associated with the granule fusion process (or upstream calcium responses) and does not require a glucose-dependent step. We show that F-actin coating depends on branched chain Arp2/3 nucleation, with evidence that it is likely to be recruited as part of the endocytic machinery. Inhibition of Arp3 activity, either through drugs or by short hairpin RNA (shRNA) blocks F-actin coating, leads to a trapping of fused granules at the cell membrane and inhibits insulin secretion. In contrast, block of linear nucleation dramatically shortens granule lifetimes but has no effect on insulin secretion. We conclude that actin coating of granules is intimately involved in the control of insulin granule dynamics and insulin secretion.

RESULTS

Dispersed endocrine cells from islets isolated from transgenic mice expressing Lifeact-GFP (Riedl et al., 2008) were imaged using two-photon microscopy. Lifeact-GFP has low-affinity binding for F-actin and the fluorescent signal; therefore, highlights F-actin, which, in these cells, is enriched in the subcortical region and in motile filopodia. We specifically focused the image plane along the cell/coverslip interface, which, in experiments with fluorescent beads, gave a measured effective image depth of ∼600 nm. As a result of this image depth, our images of cells expressing Lifeact-GFP show bright signals in cells close to the coverslip and dimmer signals in cells further away (see Figs 1, 3, 6, 7). Increasing glucose from 3 mM to 15 mM for ∼20 min failed to induce any major change to the overall distribution of F-actin, which remained enriched subcortically (Fig. 1A). Furthermore, even at 2 min after glucose stimulation, we did not see any significant changes in F-actin, as might be expected if the subcortical actin had to be remodelled to allow granules to fuse with the plasma membrane (Fig. 1A). However, we did observe the formation of very small
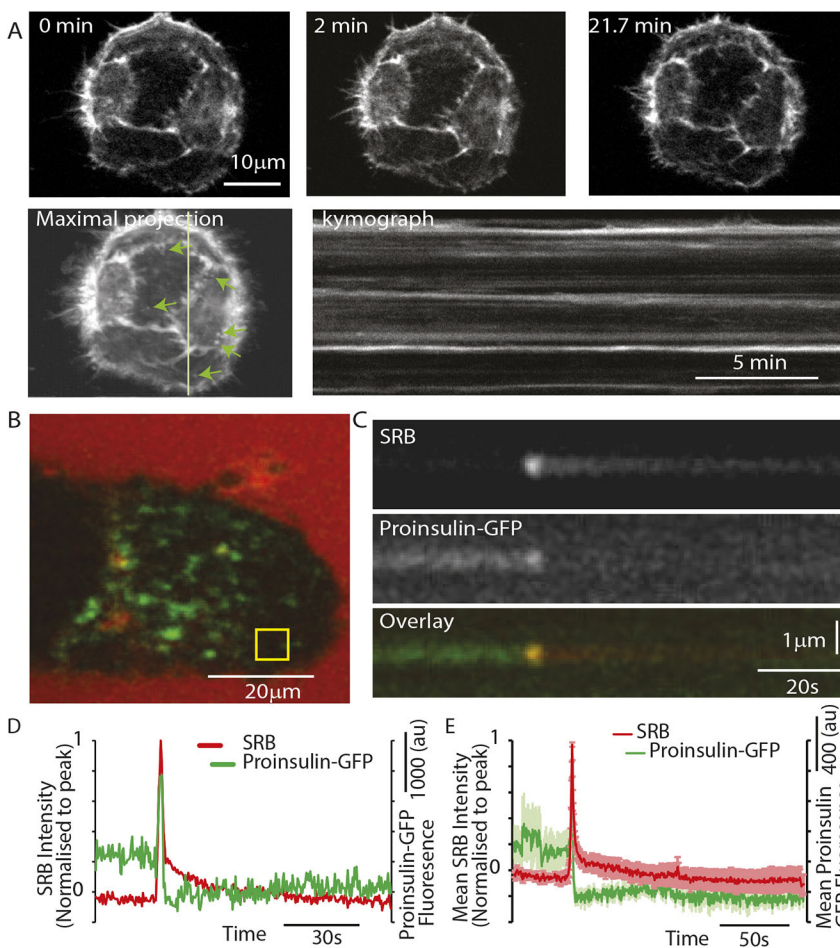

Fig. 1. Overall F-actin shows no major remodelling in response to glucose. (A) Low-magnification live-cell two-photon image of a cluster of dispersed islet cells from Lifeact-GFP transgenic animals, showing fluorescence in the subplasmalemmal region of each cell and in microfilaments projecting from the cells. The cells were stimulated for 21.7 min in 15 mM glucose and little overall change was observed after 2 min, or at the end of stimulation. A kymograph recording of fluorescence over time along a line (shown in yellow on the maximal projection) confirmed no substantial change in F-actin. However, maximal projections showed evidence for F-actin changes as small spots (arrows) across the cells. (B) Low-magnification two-photon image of a cluster of dispersed islet cells expressing proinsulin-GFP (green) and bathed in SRB (red). (C) Cells were stimulated with 15 mM glucose, and kymograph images, taken from the region of interest shown in B, show fluorescence changes over time across a line drawn through a single granule fusion event. (D) The same event as in C, showing fluorescence changes over time within a region of interest drawn over the fusing granule. (E) An average of 18 exocytic events (six animals), showing mean±s.e.m. changes in SRB and proinsulin-GFP fluorescence over time.

(∼1 μm diameter) transient (∼50 s duration) flashes of F-actin across the subcortical region where the cells were touching the glass coverslip. These changes were obvious in the movies and in maximal projection images (Fig. 1A, arrows).

To investigate the basis of these local F-actin events in more detail we used sulforhodamine B (SRB) as an extracellular fluorescent marker of exocytosis (Ma et al., 2004; Takahashi et al., 2002; Low et al., 2013). To demonstrate the utility of this probe, we conducted experiments simultaneously, recording – using two-photon microscopy – the changes in the SRB signal associated with exocytic loss of proinsulin-GFP (Liu et al., 2007) from granules during fusion (Fig. 1B). Stimulation with 15 mM glucose led to many granule fusion events, as shown by localised sudden decreases in the proinsulin-GFP signal that were often preceded by a bright flash of fluorescence, presumed to be the relief of acid-quenched GFP signal (Fig. 1C,D) (Tsuboi et al., 2004). The time points of these proinsulin-GFP changes, for all events, were always marked by a sudden increase in the SRB signal, indicative of SRB entering the fusing granule (Fig. 1D,E). Subsequent to granule fusion the insulin-GFP signal did not change consistently, but the SRB signal showed a biphasic decline, as observed previously (Takahashi et al., 2002; Low et al., 2013). These changes are consistent with a loss of granule content, as measured with proinsulin-GFP, and then collapse of the granule into the plasma membrane, as measured by the SRB signal. We conclude that SRB

is an excellent marker of granule behaviour, both as an indicator of initial fusion and then to follow granule behaviour after fusion.

Simultaneous two-photon imaging of Lifeact-GFP and extracellular SRB demonstrated that all of the 15 mM glucose-induced small, transient Lifeact-GFP changes were associated with exocytic events, as marked with SRB responses (Fig. 2A–D). Note that these cells are endocrine cells and not positively identified specifically as β cells. However, in the mouse, 90% of islet cells are β cells (Dolenšek et al., 2015) and these are the only cells that respond to glucose with an increase in granule fusion (Ashcroft and Rorsman, 2012). While we cannot exclude the possibility that some granule fusion events identified by SRB are not insulin granules, the vast majority will be (Low et al., 2013). All events, identified with SRB, had biphasic decay lifetimes with the second phase being very variable (Fig. 2E,F). This indicates that some granules rapidly collapse into the cell membrane, whereas others stay at the cell membrane. We observed these different lifetimes in control and Lifeact-GFP-expressing cells, indicating that this is normal post-fusion granule behaviour. Interestingly, the SRB peak always preceded the change in F-actin, which reached a peak ∼10 s after the SRB peak and then decayed over ∼50 s (Fig. 2B–D). As a control, we also measured insulin secretion from islets isolated from Lifeact-GFP animals and showed glucose-dependent secretion comparable with control responses (Fig. 2G), indicating that Lifeact itself is not interfering with exocytic secretion (Jang et al., 2012). Local
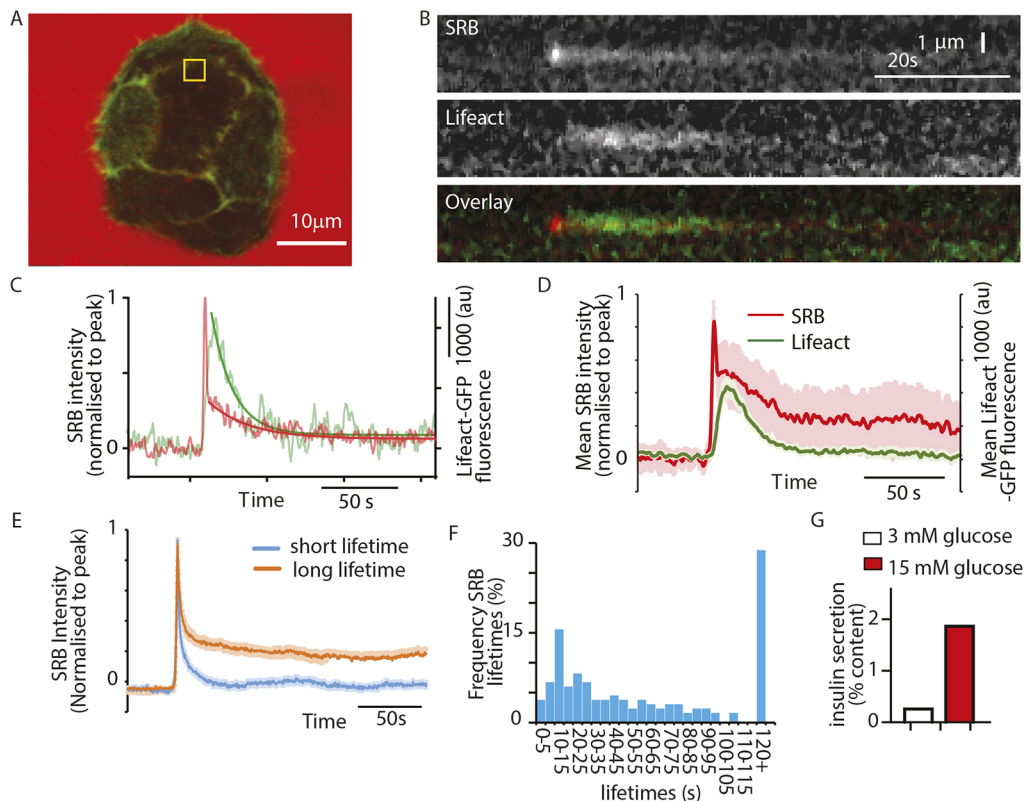

Fig. 2. Insulin granule fusion is closely associated in space and time with transient F-actin events. (A) Low-magnification fluorescence image (red, SRB; green, Lifeact-GFP) of a cluster of cells dispersed from isolated islets. (B) Cells were stimulated with 15 mM glucose, and kymograph images, taken from the region of interest shown in A, show fluorescence changes over time across a line drawn through a single granule fusion event. The sudden appearance of a bright spot of SRB fluorescence is followed by a slower, and transient, rise in Lifeact-GFP fluorescence. (C) The same data as in B, obtained using a region of interest placed over the fusing granule. The solid red and green lines represent the best fit of a single exponential decay fitted to the slow component of the SRB signal and the decay of the Lifeact-GFP signal (n=16 events). (D) An average of 30 exocytic events (from three animals), showing the mean±s.e.m. fluorescence changes over time during granule fusion. (E) An average of 154 events (from 22 animals; mean±s.e.m.), comparing events of less than 120 s duration (short lifetime, defined as the time to decrease to a threshold <2× the s.d. of the noise) with events longer than 120 s. (F) Frequency lifetime distribution for all events. (G) Insulin secretion from islets isolated from Lifeact-GFP-expressing mice in response to 15 mM glucose.
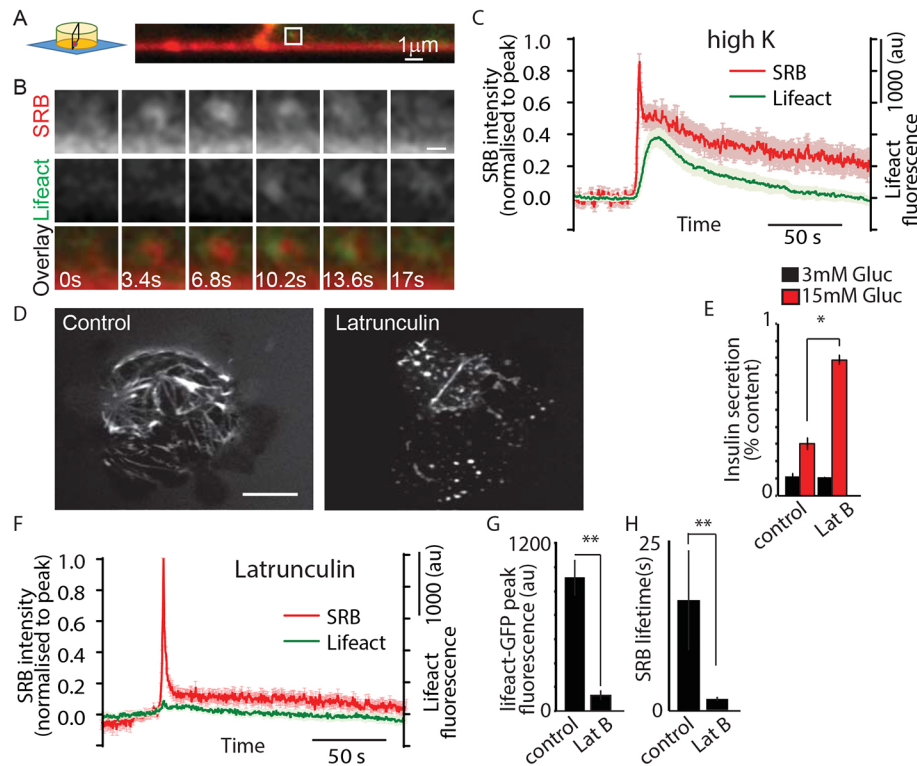
Fig. 3. Characterisation of the F-actin changes associated with granule fusion. (A) XZt confocal imaging showing the interface of the bottom of a cell with the SRB extracellular dye (red). (B) A sequence of XZ images over time, taken from the region of interest shown in A, showing that the sudden appearance of a spot of SRB fluorescence, indicating granule fusion, is followed by a coating of the granule with Lifeact-GFP. (C) Granule fusion events induced by 50 mM potassium stimulation (potassium substituted 1:1 with sodium) show SRB and Lifeact-GFP fluorescence changes similar to those induced by glucose (average of 31 exocytic events; three animals; mean±s.e.m.). (D) F-actin, as shown by Lifeact-GFP, is disrupted (compared to the control) by treatment with latrunculin. Scale bar: 10 µm. (E) Glucose-dependent insulin secretion, in the presence of latrunculin, was significantly increased. *$P<0.05$, Student's t-test, $n=5$ control, $n=7$ latrunculin islet preparations. (F) Treatment with 1 µM latrunculin for 30 min and then stimulation with 15 mM glucose triggered numerous granule fusion events with very small changes in the Lifeact-GFP signal and shorter SRB events ($n=70$ events). (G) The peak Lifeact-GFP signal was significantly reduced by latrunculin treatment ($n=70$ events with latrunculin compared to $n=30$ control events, Student's t-test, **$P<0.001$). (H) The SRB lifetime (time to 50% decay) in the presence of latrunculin was significantly reduced ($n=54$ events with latrunculin compared to $n=28$ control events, Student's t-test, **$P<0.01$).

changes in F-actin have been observed after granule fusion in cell types with larger granules (Sokac et al., 2003), and, although F-actin changes have been occasionally seen in the endocrine chromaffin cells (Wen et al., 2016), this is the first report in β cells. Importantly, we show that the F-actin changes occur for all fusing granules, indicating that they are essentially coupled with exocytosis.

What are the characteristics of the F-actin changes at the sites of granule fusion?

To define these local F-actin changes, we first tested whether they encircle the granule or are restricted to the subcortical region. Using 3D confocal microscopy, we imaged XZt sections along the interface of the cell with the glass coverslip (Fig. 3A,B). This showed that 15 mM glucose-induced granule fusion events, as indicated by SRB entry, were associated with an encircling of the granule by F-actin, which is consistent with previous reports from cell types with larger granules (Fig. 3B).

We next tested whether the F-actin changes were specific to glucose as a stimulus since previous reports in β cells provide evidence that glucose can induce selective activation of F-actin polymerisation (Wang et al., 2007; Uenishi et al., 2013). Using high potassium as a stimulus, we observed many fusion events, recorded using SRB entry into the granule, and, for each of these, we observed local, transient changes in F-actin that were indistinguishable from those induced in the presence of high glucose (Fig. 3C). We conclude

that initiation of the local F-actin changes is induced either by the calcium rise or the granule fusion event, and that alternative pathways, dependent on glucose, are not necessary.

In principle, the local changes in F-actin at the sites of granule fusion could be due to *de novo* actin polymerisation or F-actin movement and reshaping. To test these possibilities, we incubated the cells in 1 µM latrunculin, which sequesters monomeric actin and prevents the formation of F-actin (Mourad et al., 2010; Orci et al., 1972). Compared to the control condition, treatment with latrunculin almost abolished F-actin filaments, leaving a few large blobs of F-actin cross the cells (Fig. 3D). Furthermore, consistent with previous reports (Mourad et al., 2010), we show that latrunculin pretreatment increased glucose-induced insulin secretion (Fig. 3E).

Glucose stimulation of the cells, in the presence of latrunculin, led to many granule fusion events, as measured with SRB, but now the events were not associated with any change in F-actin, indicating that actin polymerisation is the key step in the F-actin changes at the site of granule fusion (Fig. 3F,G). Interestingly, the SRB signal also changed and was shorter, with a reduction in the slower second phase of decay (Fig. 3F,H). This suggests that, in the absence of the F-actin coat, the granules are unstable and collapse quicker into the plasma membrane. Given that latrunculin has a global effect on F-actin, we expect it to weaken the subcortical pool and this will affect membrane tension (Wen et al., 2016), which could also cause granule instability.

The number of fusion events recorded by SRB is proportional to the amount of insulin secretion (Low et al., 2013). Using 15 mM glucose, in control experiments, we observed 10.4±2.6 fusion events/cell cluster/20 min (mean±s.e.m., n=16) and with latrunculin, 45.8±4.3 fusion events/cell cluster/20 min (mean± s.e.m., n=5), demonstrating a significant increase in fusion events (Student's t-test, P<0.01). This suggests that the increased insulin secretion observed with latrunculin treatment is primarily due to an increase in the number of fusion events and not on the event kinetics.

The effect of latrunculin to abolish F-actin coating indicates that these F-actin changes are mediated by actin polymerisation, leading to F-actin remodelling right around the granule. This actin polymerisation is triggered directly by the exocytic process and is not dependent on any other glucose-dependent factor.

Granule fusion is associated with local enrichment of Arp3

Our data using latrunculin imply that actin nucleation is the major mediator of granule coating. Actin polymerisation occurs either by linear or branched addition of actin monomers, with both processes nucleated by distinct effectors. Branched chain polymerisation is nucleated by the Arp2/3 complex and has been implicated in F-actin remodelling around larger granules. To test for this role in β cells, we expressed Arp3-GFP in the MIN6 β-cell line (using stable lentiviral expression). At rest, Arp3-GFP was located throughout the cytosol (Fig. 4A) and in puncta at the cell membrane. This overall distribution did not significantly change during 15 mM glucose stimulation (see Fig. 4A, image at 2 min after stimulation). However, we did observe local, specific recruitment to the fusing granules (Fig. 4B–D). Arp3-GFP fluorescence increased rapidly after granule fusion, identified by the SRB peak, and then remained within the region (Fig. 4C,D). The mean signal (Fig. 4E) indicates that Arp3-GFP did eventually decay back to baseline, and, because this is the time course over which the granule is collapsing, this suggests that the Arp2/3 complex is recruited to the fusing granule

and then remains with the F-actin network as the granule collapses into the plasma membrane.

Granule fusion is associated with the early recruitment of the endocytic machinery

There are many processes upstream of Arp2/3 that recruit the complex and then activate it to polymerise actin. One of these processes is the endocytic machinery, in which Arp2/3-dependent F-actin polymerisation is an essential step for endocytosis in many systems (Almeida-Souza et al., 2018). Intriguingly, dynamin 2 has previously been shown to be recruited by insulin granules during granule fusion (Tsuboi et al., 2004). To study the time course of recruitment, we expressed dynamin 2-GFP (using a lentiviral vector) in MIN6 β cells. Dynamin 2-GFP was observed in resting cells as puncta across the cell membrane (Fig. 5A), and, after stimulation with 15 mM glucose, exocytic events marked by changes in SRB were associated with local enrichment of dynamin 2-GFP (Fig. 5B–D). This dynamin 2 recruitment occurred rapidly after the SRB peak and was transient, indicating dynamic changes over the lifetime of the granule. We conclude that dynamin 2, one of the key drivers of endocytosis, is recruited very rapidly after granule fusion and before the granule collapses into the cell membrane.

To further test the observation of the early recruitment of the endocytic machinery, we expressed clathrin light chain-GFP (clathrin-GFP) using an adenoviral probe in isolated native β cells. Previous work indicates that clathrin is recruited rapidly after insulin granule fusion (Yuan et al., 2015), although it is unknown if this is before or after granule collapse. At rest, clathrin-GFP appeared in punctate spots at the cell periphery (Fig. 5E), and, after glucose stimulation, it too was recruited close to each fusing granule (Fig. 5F–H). An interesting observation was that for many fusing events we observed a clear drop in the clathrin-GFP signal at exactly the time point of granule fusion (Fig. 5G). This suggests that, prior to fusion, the granules do not have clathrin, and as they fuse, they
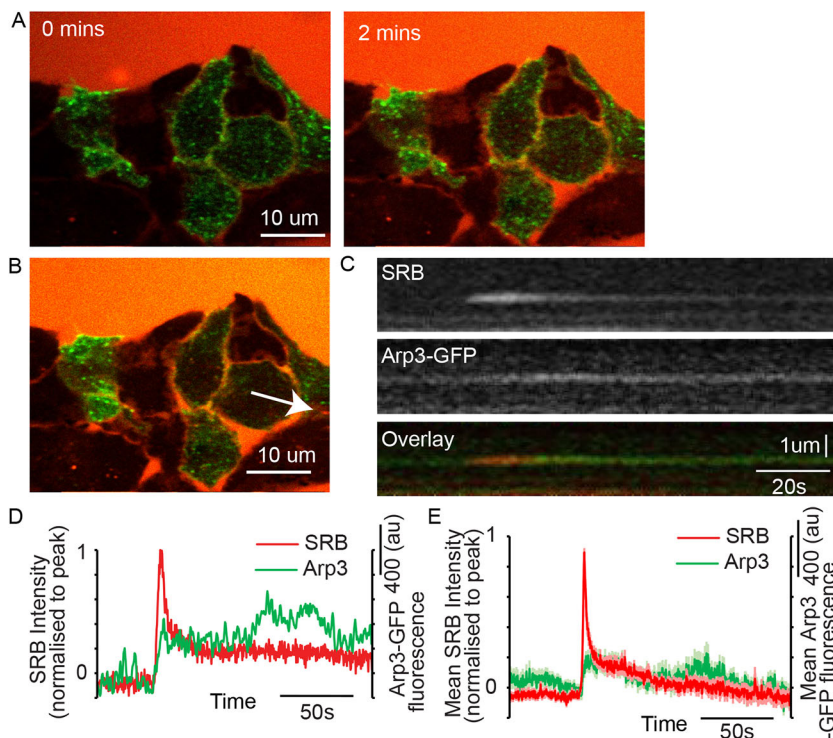

Fig. 4. Arp3 is rapidly recruited to the sites of granule fusion. (A) Low-magnification fluorescence image (red, SRB; green, Arp3-GFP) of a cluster of MIN6 cells, which does not change significantly after 2 min of 15 mM glucose stimulation. (B) Low-magnification fluorescence image (red, SRB; green, Arp3-GFP) of a cluster of MIN6 cells. (C) Kymograph images, taken from an event marked with the arrow in B, showing fluorescence changes over time across a line drawn through a single granule fusion event. The sudden appearance of a bright spot of SRB fluorescence is followed by a rapid rise in Arp3-GFP fluorescence. (D The same data as in C, obtained using a region of interest placed over the fusing granule. (E) An average of 26 exocytic events (from four independent experiments), showing the mean±s.e.m. fluorescence changes over time during granule fusion.
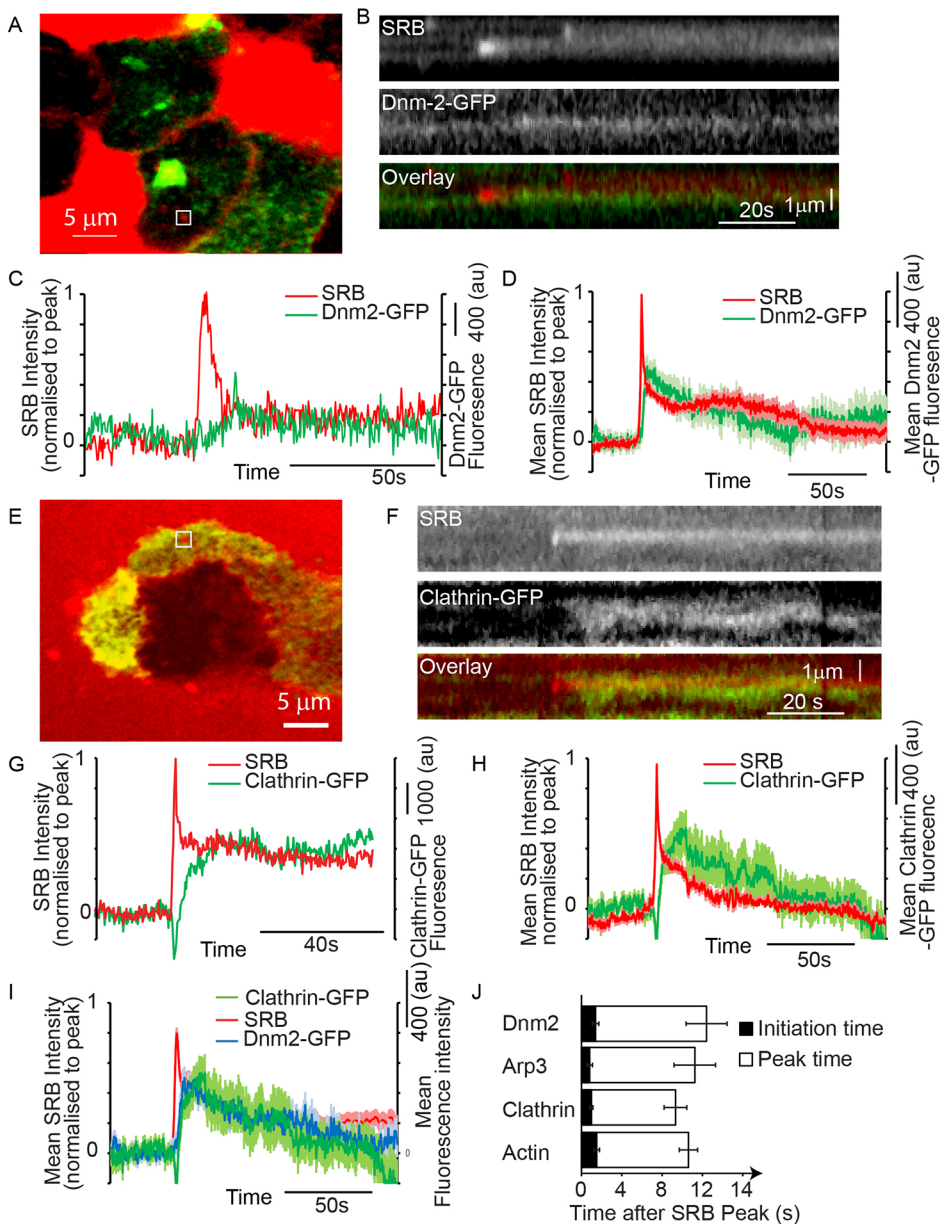
Fig. 5. Recruitment of endocytic machinery to the sites of granule fusion. (A) Low-magnification fluorescence image (red, SRB; green, dynamin 2) of a cluster of MIN6 cells. (B) Kymograph images, taken from the region of interest shown in A, showing fluorescence changes over time across a line drawn through a single granule fusion event. The sudden appearance of a bright spot of SRB fluorescence is followed by a rapid rise in dynamin 2-GFP (Dnm-2-GFP) fluorescence. (C) The same data as in B, obtained using a region of interest placed over the fusing granule. (D) An average of 24 exocytic events (three independent experiments), showing the mean± s.e.m. fluorescence changes over time during granule fusion. (E) Low-magnification fluorescence image (red, SRB; green, clathrin-GFP) of a cluster of cells dispersed from isolated islets. (F) Kymograph images showing fluorescence changes over time across a line drawn through a single granule fusion event. The sudden appearance of a bright spot of SRB fluorescence is followed by a delayed, and transient, rise in clathrin-GFP fluorescence. (G) The same data as in F, obtained using a region of interest placed over the fusing granule. (H) An average of 34 exocytic events (six animals), showing the mean±s.e.m. fluorescence changes over time during granule fusion. (I) Overlay of the mean±s.e.m. of the fluorescence signal over time for clathrin-GFP and dynamin 2-GFP, both aligned with the rising phase of the SRB signal. Note that these overlays combine the data obtained from native cells and the MIN6 cell line. (J) Histogram showing the time of initiation (fluorescence deviation of >2× s.d. of the noise) and peak fluorescence, with respect to the SRB rising phase for dynamin 2-GFP (n=18 events), Arp3-GFP (n=25 events), clathrin-GFP (n=27 events) and Lifeact-GFP (n=30 events).

clear clathrin from the plasma membrane and then, after fusion, clathrin is recruited back to the granule. Further experimentation would be required to prove this, but the local enrichment of dynamin 2 and clathrin (Fig. 5I,J) strongly suggests that the endocytic machinery is rapidly recruited after fusion and is decorating a granule that is still fusing.

Arp2/3-dependent F-actin coating drives insulin secretion
Our work indicates that Arp3 is recruited to the fusion granule possibly in association with the endocytic machinery. To test whether Arp2/3 is the major driver of F-actin coating around the granules, we pretreated β cells with 100 μM CK666, an Arp2/3 inhibitor (Yang et al., 2012; Wu et al., 2012), prior to 15 mM glucose stimulation. We observed that CK666 had a modest effect on F-actin structures and subcortical F-actin was still apparent (Fig. 6A). In response to glucose, granule fusion events were still observed, but these now occurred in the complete absence of any change in the Lifeact-GFP signal, indicating that actin polymerisation had been prevented (Fig. 6B–E). Furthermore, the

CK666 treatment has a dramatic effect on the SRB signal, and, after granule fusion, for many events the signal completely failed to decay, indicating that the granules remain at the cell surface (Fig. 6B–E). Neither the effect on Lifeact-GFP nor the effect on SRB lifetimes were observed with CK689, the inactive analogue of CK666 (Fig. 6F). These profound effects on granule behaviour suggest an impact on insulin secretion and, indeed, when tested, we observed a significant reduction in insulin secretion with CK666 treatment but not with CK689 (Fig. 6G), and also with shRNA against Arp3 (lentiviral expression in MIN6 β-cell line) (Fig. 6H–J). Together these results point to an intimate link between Arp2/3-dependent F-actin dynamics, granule behaviour and the control of insulin secretion.

In principle, the reduction of insulin secretion with CK666 could be due to the action of the drug to inhibit the number of granule fusion events. With 15 mM glucose, our control experiments recorded 10.4±2.6 fusion events/cell cluster/20 min (mean±s.e.m., n=16); with CK666 we recorded 6.0±1.6 fusion events/cell cluster/ 20 min (mean±s.e.m., n=8) and with CK689 we recorded 7.8±
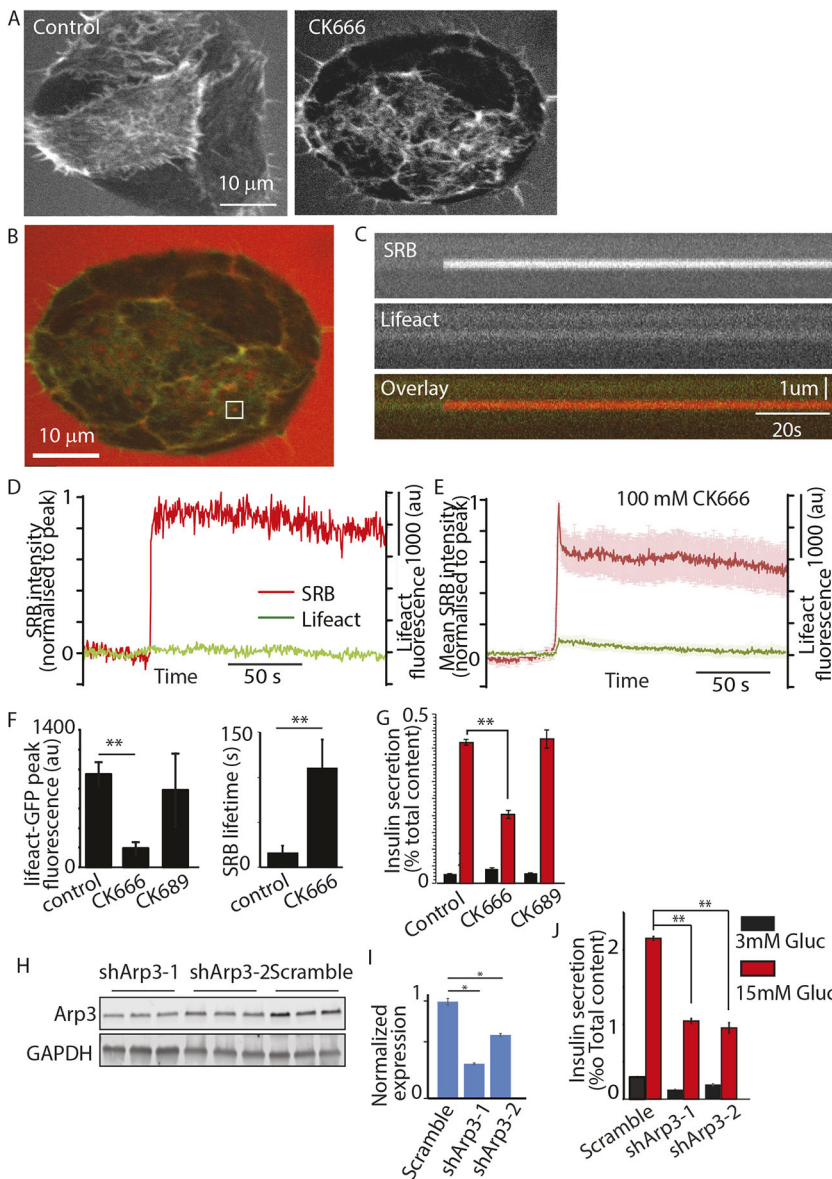
Fig. 6. Branched actin nucleators affect granule fusion and insulin secretion. (A) Low-magnification image of Lifeact-GFP, showing that CK666 affects the pattern of F-actin in a cell cluster. (B) Low-magnification fluorescence image (red, SRB; green, Lifeact-GFP) of a cluster of cells dispersed from isolated islets bathed in 100 μM CK666. (C) Kymograph images, taken from the region of interest shown in B, showing fluorescence changes over time across a line drawn through a single granule fusion event. In the presence of CK666, the sudden appearance of a bright spot of SRB fluorescence is no longer followed by any change in Lifeact-GFP. (D) The same data as in C, obtained using a region of interest placed over the fusing granule to measure changes in fluorescence over time. (E) An average of 49 exocytic events (nine animals), in the presence of CK666, showing the mean±s.e.m. fluorescence changes over time during granule fusion. (F) CK666, but not CK689, significantly inhibits the Lifeact-GFP peak fluorescence [glucose vs CK666, two-tailed Student's t-test, **$P<0.01$ ($n=30$ control, 26 CK666 events), glucose vs CK689, two-tailed Student's t-test, $P=0.6$ ($n=15$ CK689 events)]. CK666 significantly increases the average granule lifetimes, as measured with SRB (two-tailed Student's t-test, $P<0.01$; $n=24$ control, 28 CK666 events). (G) Insulin secretion in response to 15 mM glucose was significantly reduced in the presence of CK666 ($n=8$ replicates, Student's t-test, **$P<0.01$) and not in the presence of CK689 ($n=8$ replicates, Student's t-test, $P=0.97$). (H–J) Compared to scrambled probe shRNA against Arp3 (shArp3-1 and shArp3-2), lentiviral expression in MIN6 cells induced knockdown of protein, as shown in western blot analysis (H), quantified to reveal reduction of Arp3 with shArp3-1 to 35%, and shArp3-2 to 66%, of scramble control (Student's t-test, *$P<0.05$) (I), and significant reductions in 15 mM glucose-induced secretion (all conditions $n=9$ replicates, Student's t-test for both shRNA species, **$P<0.01$) (J).

1.8 fusion events/cell cluster/20 min (mean±s.e.m., $n=6$). This indicates there are no significant changes in the number of fusion events with CK666 (Student's t-test, $P=0.26$ compared to control, $P=0.47$ compared to CK689) suggesting that the decreased insulin secretion observed with CK666 treatment is due to the effect on the event kinetics.

In addition to Arp2/3-dependent branched chain polymerisation, the other mechanism for actin polymerisation uses formins as linear nucleators, and, to test their role, we used the specific blocker SMIFH2 (Rizvi et al., 2009). Pretreatment with 50–100 μM SMIFH2 led to an apparent reduction in F-actin and a change in F-actin distribution, with the appearance of tangled filaments (Fig. 7A). In response to glucose stimulation, granule fusion was still observed with SRB but there was a significant reduction in the local changes in Lifeact-GFP (Fig. 7B–E). However, in contrast to Arp2/3 inhibition, the SRB signal was significantly shorter, which is similar to the effects of latrunculin (Fig. 7B–E). Furthermore, SMIFH2 failed to have any effect on glucose-induced insulin secretion (Fig. 7E). Consistent with this, the number of fusion events was not altered with SMIFH2 treatment. With 15 mM

glucose, our control experiments recorded 10.4±2.6 fusion events/cell cluster/20 min (mean±s.e.m., $n=16$); with SMIFH2, we recorded 18±17.2 fusion events/cell cluster/20 min (mean±s.e.m., $n=6$), which was not significantly different (Student's t-test, $P=0.22$ compared to control).

The fact that inhibition of branched and linear chain actin polymerisation both led to loss of F-actin coating of granules demonstrates a requirement for both mechanisms. However, the opposite phenotype in terms of the kinetics of SRB signal and insulin secretion indicates distinct effects. The shorter lifetimes induced by formin inhibition suggest granule instability, and, given that the same effect is observed with latrunculin, this probably arises due to loss of subcortical linear F-actin. In contrast, inhibition of Arp2/3 leads to fused granules trapped at the cell membrane, suggesting that F-actin plays an active role in the processes after granule fusion and granule collapse.

DISCUSSION
Our data show localised and transient F-actin remodelling around each fusing granule in pancreatic β cells. Our evidence, using high
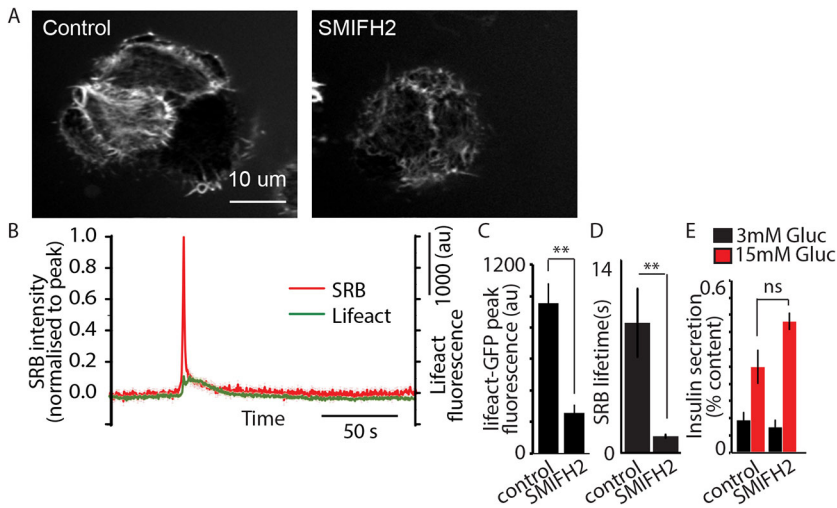
Fig. 7. Linear actin nucleators alter granule dynamics but do not affect secretion. (A) Low-magnification image of Lifeact-GFP showing that SMIFH2 affects the amount and pattern of F-actin in a cell cluster. (B) Pretreatment for 30 min with 50 μM SMIFH2 and then stimulation with 15 mM glucose induced many granule fusion events with short SRB lifetimes and small changes in Lifeact-GFP (n=25 events). (C) The peak Lifeact-GFP signal was significantly smaller (n=25 events with SMIFH2, n=30 control events; Student's t-test, P<0.01). (D) The SRB lifetime was significantly shorter in the presence of SMIFH2 (n=25 events with SMIFH2, n=28 control events; Student's t-test, P<0.001). (E) SMIFH2 had no significant effect on 15 mM glucose-stimulated secretion (Student's t-test, n=8 replicates). ns, not significant.

potassium as a stimulus, indicates that the F-actin coating of granules is dependent primarily on the granule fusion process itself, including possibly the calcium response, and does not require a specific glucose-dependent signal. We show that the F-actin changes lead to a coating of the granule and are coincident with local enrichment of the endocytic proteins dynamin 2 and clathrin, which occurs quickly after granule fusion. Using inhibitors and shRNA against Arp3, we demonstrate that F-actin remodelling is dependent on Arp2/3 branched chain polymerisation, and that reduction of Arp2/3 activity traps fusing granules at the cell membrane and significantly inhibits glucose-dependent insulin secretion. Our analysis shows that Arp2/3 inhibition does not affect the numbers of granules fusing in response to glucose and therefore the reduction in insulin secretion may be the direct result of the altered granule kinetics.

Interestingly, latrunculin and SMIFH2 also affect granule dynamics; both decrease the SRB lifetimes, indicating that the granules are unstable and collapse rapidly into the cell membrane. However, latrunculin must have an additional action because we observe a significant increase in the number of fusion events compared to control with latrunculin but not with SMIFH2. One possibility is that the almost complete removal of F-actin with latrunculin (see Fig. 3D) allows uncontrolled access of granules to the cell membrane. In contrast, after SMIFH2 treatment, F-actin structure is still present and could be a sufficient barrier to prevent granule access to the cell membrane.

How do the different forms of actin nucleation control granule behaviour?

The contrasting effects of branched versus linear chain actin nucleators on granule dynamics suggest distinct sites of action. We propose that the loss of subcortical linear F-actin with latrunculin and SMIFH2 affects the stability of the fusion pore, leading to uncontrolled pore dilation and granule collapse. In contrast, block of branched chain polymerisation prevents F-actin coating and traps the granules at the cell surface. This occurs either because F-actin plays a role in squeezing and the collapse of the granule, as proposed in other systems (Nightingale et al., 2011; Rousso et al., 2016), or because the fusion pore closes (Larina et al., 2007). Recent methods are enabling real-time measurement of pore closure (Chiang et al., 2014), and applied to β cells these would help to resolve whether the 'trapped' granules we see in response to Arp2/3 inhibition have open or closed fusion pores. We note here that there may be other forms of post-fusion granule

behaviour, such as shrink fusion, where the fusion pore appears stable (i.e. does not dilate) but the granules still merge with the plasma membrane (Chiang et al., 2014). Although it is not known, our evidence for F-actin coating of each fused granule means the microfilaments are centrally placed to control any form of post-fusion behaviour.

Our conclusion that different forms of nucleation have different functional actions can only be tentative because of two outstanding problems. The first is that the activity of the nucleators is necessarily interdependent. Both nucleators depend on pre-existing F-actin and so without a scaffold of linear F-actin the branched chain nucleator Arp2/3 cannot work. Second, there is a further complication in that the action of both nucleators is limited by the supply of monomeric actin (Suarez and Kovar, 2016). As a result, inhibition of one form of nucleation can paradoxically enhance the other. Notwithstanding these complications in the precise mechanism, it is clear that both nucleators control granule behaviour and, in the case of Arp2/3, act to control insulin secretion.

The lack of evidence for glucose-dependent changes in F-actin might suggest that the local F-actin dynamics around the granule are not part of the normal mechanism to control secretion. However, once in place, the F-actin coat could be a target for glucose-dependent control. For example, the major regulator of myosin II is calcium (Somlyo and Somlyo, 2003), and the oscillatory calcium responses induced by glucose could control myosin contractility to mediate effects on granule or fusion pore behaviour. In addition, we show a temporal and spatial association between Arp3 and the endocytic machinery, suggesting that actin nucleation may be part of the endocytic process as observed in other systems (Sun et al., 2015; Almeida-Souza et al., 2018). Overall, our evidence that inhibiting Arp3 activity does affect insulin secretion firmly places the local F-actin changes around the granule as functionally significant.

How do our observations relate with previous work on F-actin in β cells?

Glucose-dependent F-actin changes have previously been identified in pancreatic β cells; Cdc42 (Wang et al., 2007) and WASP (Uenishi et al., 2013) have been shown to be specifically activated by glucose stimulation and are thought to affect the cortical F-actin web. It is clear that wherever these glucose-dependent changes occur, they are not intimately linked with the local F-actin granule coating we observe, because we see the same coating when high potassium is used as a stimulus. Instead, it is more likely that the glucose-dependent effects previously identified precede granule fusion and

play a role in pre-fusion granule mobility (Heaslip et al., 2014) and transport to the cell periphery (Orci et al., 1972).

Close similarities between our observations and those in cells types with large granules

The close similarities between our data and the data on exocrine cells (Jang et al., 2012; Tran et al., 2015; Rousso et al., 2016; Miklavc et al., 2012) and oocytes (Sokac et al., 2003) are striking. In all cases, F-actin nucleation takes place after granule fusion and is dependent on actin nucleation, and F-actin coats the granules as they fuse. Evidence from other cell types also shows that that the trigger for nucleation is granule fusion itself (Gasman et al., 2004; Yu and Bement, 2007), consistent with our findings in β cells. The models for nucleation highlight the importance of the spatial changes that occur during granule fusion and suggest that fusion brings together components on the granule with components at the cell membrane (Gasman et al., 2004; Sokac and Bement, 2006). These can then form competent and activated complexes for F-actin nucleation that arise only on the fusing granule and so explain the spatial and temporal specificity of F-actin coating.

The conservation of F-actin coating in these different cell types suggests that it plays a fundamental role in the behaviour of granules after fusion. One proposed role is the squeezing out of granule content by contraction of the F-actin coat (Sokac et al., 2003; Nightingale et al., 2011), with evidence for a dependence on myosin (Nightingale et al., 2011; Rousso et al., 2016). Another role is in the control of the fusion pore, as there is evidence that F-actin (Larina et al., 2007) and myosin (Doreian et al., 2008; Ñeco et al., 2008) provide force around the pore to affect its behaviour. Distinguishing between these possibilities is difficult because prevention of either leads to the same consequence of granules trapped at the cell surface. Specific techniques, such as content photobleaching (Larina et al., 2007; Miklavc et al., 2012), can be used to assay whether a pore is open or closed, and, consistent with earlier electrophysiological data (Fernández-Peruchena et al., 2005), these show that the pore dynamically opens and closes (Shin et al., 2018). Given that the fusion pore forms at the interface of the granule and the subcortical F-actin network, we would expect to see complex effects and interactions. Our data showing that latrunculin and SMIFH2 both lead to unstable granules that collapse into the cell membrane support the idea that a pool of F-actin, dependent on linear nucleation, is responsible for maintaining the integrity of the pore during fusion.

Conclusions

Our work identifies a precise site of action for F-actin in the stimulus-secretion pathway of pancreatic β cells. We define the local activation of actin nucleators to provoke a transient F-actin coat around individual fusing granules in pancreatic β cells. We show that inhibition of Arp2/3 nucleation significantly reduces insulin secretion, demonstrating the functional significance in the control of this essential cell behaviour.

MATERIALS AND METHODS

Islet isolation and dispersion

C57BL/6 or Lifeact male mice aged between 8 and 12 weeks were maintained under normal diets under standard animal housing conditions. Mice were humanely killed according to the local animal ethics procedures (approved by the University of Sydney Research Integrity and Ethics Administration Committee, project #2015/908) and complying with local animal welfare laws, guidelines and policies. Isolated mouse islets were obtained from the pancreas by Liberase enzyme digestion (Roche, Liberase TL). Isolated islets were separated from the cell debris using the Histopaque

cell-density-gradient layering method (Sigma-Aldrich, Histopaque #1077 and #1119). Primary β cells were prepared by digesting isolated islets with TrypLE express enzyme (Gibco) and cultured in RPMI-1640 (Gibco), supplemented with 10% fetal bovine serum (FBS; Gibco) and 100 U/ml penicillin-0.1 mg/ml streptomycin (Life Technologies) in standard incubator conditions (37°C, 95/5% air/CO$_2$). Where indicated, wild-type β cells were infected with adenovirus to express either proinsulin-emerald or clathrin-GFP. The cells were incubated overnight and imaged.

Mouse insulinoma (MIN6) cells were maintained in Dulbecco's modified eagle medium (DMEM), supplemented with 15% FBS, 1% penicillin-streptomycin and 0.05 mM 2-mercaptoethanol under standard culture incubator conditions (37°C, 95/5% air/CO$_2$). The MIN6 cells were infected with lentivirus expression Arp3-GFP or dynamin 2-GFP and subjected to two-photon microscopy imaging.

Virus generation and infection

Lentiviruses were produced by co-transfecting lentiviral expression and packaging plasmids into HEK-293T cells by the polyethylenimine transfection method. Virus-containing medium was collected 48 h after transfection followed by centrifugation at 1000 g for 4 min and filtered through a 0.45 µm filter. To generate a stable MIN6 cell line, the cells were cultured in virus-containing medium for 12 h, then replaced with fresh DMEM. The cells were then cultured for 2 more days prior to imaging. The Lenti-Arp3-GFP, Lenti-dynamin 2-GFP expression vectors were purchased from Origene (MR217895L2, RC223585L2). Proinsulin-GFP was produced using a vector from Weiping Han, Singapore Bioimaging Consortium, A*STAR, Singapore.

Adenovirus was generated by transfecting linearised adenoviral vectors into HEK-293A cells through the polyethylenimine transfection method. The transfected cells were cultured for 7–10 days. Adenovirus was harvested from the cell lysate by freeze-thaw. Cultured primary β cells were subjected to adenoviral infection for 16 h, then replaced with fresh RPMI. Adeno-Proinsulin-Emerald vector was cloned using a pAdEasy system (Agilent). Adenovirus clathrin-GFP was customised and purchased from Vector Biolabs.

Live-cell imaging

Live-cell experiments were performed in Na-rich extracellular buffer (ECM buffer) (ECM buffer) (140 mM NaCl, 5 mM KCl, 1 mM MgCl$_2$, 2.5 mM CaCl$_2$, 5 mM NaHCO$_3$, 5 mM HEPES, 3–25 mM glucose), adjusted to pH 7.4 with NaOH. Islet β cells were cultured in RPMI medium overnight and, prior to imaging, were bathed in an extracellular solution containing 3 mmol/l glucose for 30 min (37°C, 95/5% air/CO$_2$). The buffer was supplemented with different drugs, such as CK666 or CK689 (100 µm, Sigma-Aldrich), where indicated. Two-photon imaging was taken by a home-built two-photon microscope equipped with a Chameleon multiphoton laser (950 mm) and a 60× oil objective. The confocal imaging was conducted using a Leica SP8 confocal microscope with a 93× glycerol objective at 37°C with 95/5% air/CO$_2$. The vertical section live-cell image was obtained by XZ-time scanning. The experiments were performed at 37°C with exocytic events indicated by the entry of extracellular dye (8 mM SRB) into each fused granule upon 15 mmol/l glucose stimulation.

Insulin secretion assay

Primary β cells generated from dispersed islets were cultured in RPMI medium overnight. Before imaging, primary β cells were starved in extracellular medium supplemented with 1 mg/ml bovine serum albumin, 3 mM D-glucose and 20 mM HEPES at pH 7.4 for 30 min, followed by sequential incubation in 3 mM glucose ECM buffer for 15 min and then 15 mM glucose ECM buffer for 15 min. The incubated ECM buffers were collected for measurement of insulin content. Islets were then lysed in TNET buffer for measurement of total insulin content. Sample insulin concentration was measured using a homogeneous time-resolved fluorescence (HTRF) assay (Cisbio).

Quantification and statistical analysis

All numerical data are presented as mean±s.e.m. Statistical analysis was performed using Microsoft Excel and GraphPad Prism. Image analysis was

performed in ImageJ and MetaMorph. Details of data size and statistical tests are in the figure legends. Each of the data sets was obtained from at least n=3 animals. Significance is indicated as follows: *P<0.05, **P<0.01, ***P<0.001.

Author contributions
Conceptualization: P.T., W.M., J.C., J.T., M.A.K.; Methodology: P.T., W.M., J.C., J.T., U.H., B.Y., M.A.K.; Software: P.T.; Formal analysis: P.T., J.T., U.H., B.Y.; Investigation: W.M., J.C., J.T., U.H., B.Y.; Data curation: P.T.; Writing - original draft: P.T.; Writing - review & editing: P.T., W.M., J.C., J.T., U.H., B.Y., M.A.K.; Supervision: P.T.; Project administration: P.T.; Funding acquisition: P.T.

References
Almeida-Souza, L., Frank, R. A. W., García-Nafría, J., Colussi, A., Gunawardana, N., Johnson, C. M., Yu, M., Howard, G., Andrews, B., Vallis, Y. et al. (2018). A flat BAR protein promotes actin polymerization at the base of clathrin-coated pits. *Cell* **174**, 325-337.e14. doi:10.1016/j.cell.2018.05.020

Anantharam, A. and Kreutzberger, A. J. B. (2019). Unraveling the mechanisms of calcium-dependent secretion. *J. Gen. Physiol.* **151**, 417-434. doi:10.1085/jgp.201812298

Ashcroft, F. M. and Rorsman, P. (2012). Diabetes mellitus and the β cell: the last ten years. *Cell* **148**, 1160-1171. doi:10.1016/j.cell.2012.02.010

Chiang, H.-C., Shin, W., Zhao, W.-D., Hamid, E., Sheng, J., Baydyuk, M., Wen, P. J., Jin, A., Momboisse, F. and Wu, L.-G. (2014). Post-fusion structural changes and their roles in exocytosis and endocytosis of dense-core vesicles. *Nat. Commun.* **5**, 3356. doi:10.1038/ncomms4356

Dolenšek, J., Rupnik, M. S. and Stožer, A. (2015). Structural similarities and differences between the human and the mouse pancreas. *Islets* **7**, e1024405. doi:10.1080/19382014.2015.1024405

Dominguez, R. and Holmes, K. C. (2011). Actin structure and function. *Annu. Rev. Biophys.* **40**, 169-186. doi:10.1146/annurev-biophys-042910-155359

Doreian, B. W., Fulop, T. G. and Smith, C. B. (2008). Myosin II activation and actin reorganization regulate the mode of quantal exocytosis in mouse adrenal chromaffin cells. *J. Neurosci.* **28**, 4470-4478. doi:10.1523/JNEUROSCI.0008-08.2008

Fernández-Peruchena, C., Navas, S., Montes, M. A. and Álvarez de Toledo, G. A. (2005). Fusion pore regulation of transmitter release. *Brain Res. Rev.* **49**, 406-415. doi:10.1016/j.brainresrev.2004.12.037

Gan, W. J., Zavortink, M., Ludick, C., Templin, R., Webb, R., Webb, R., Ma, W., Poronnik, P., Parton, R. G., Gaisano, H. Y. et al. (2017). Cell polarity defines three distinct domains in pancreatic β-cells. *J. Cell Sci.* **130**, 143-151. doi:10.1242/jcs.185116

Gasman, S., Chasserot-Golaz, S., Malacombe, M., Way, M. and Bader, M.-F. (2004). Regulated exocytosis in neuroendocrine cells: a role for subplasmalemmal Cdc42/N-WASP-induced actin filaments. *Mol. Biol. Cell* **15**, 520-531. doi:10.1091/mbc.e03-06-0402

Heaslip, A. T., Nelson, S. R., Lombardo, A. T., Beck Previs, S., Armstrong, J. and Warshaw, D. M. (2014). Cytoskeletal dependence of insulin granule movement dynamics in INS-1 beta-cells in response to glucose. *PLoS ONE* **9**, e109082. doi:10.1371/journal.pone.0109082

Jang, Y., Soekmadji, C., Mitchell, J. M., Thomas, W. G. and Thorn, P. (2012). Real-time measurement of F-actin remodelling during exocytosis using Lifeact-EGFP transgenic animals. *PLoS ONE* **7**, e39815. doi:10.1371/journal.pone.0039815

Larina, O., Bhat, P., Pickett, J. A., Launikonis, B. S., Shah, A., Kruger, W. A., Edwardson, J. M. and Thorn, P. (2007). Dynamic regulation of the large exocytotic fusion pore in pancreatic acinar cells. *Mol. Biol. Cell* **18**, 3502-3511. doi:10.1091/mbc.e07-01-0024

Li, P., Bademosi, A. T., Luo, J. and Meunier, F. A. (2018). Actin remodeling in regulated exocytosis: toward a mesoscopic view. *Trends Cell Biol.* **28**, 685-697. doi:10.1016/j.tcb.2018.04.004

Liu, M., Hodish, I., Rhodes, C. J. and Arvan, P. (2007). Proinsulin maturation, misfolding, and proteotoxicity. *Proc. Natl. Acad. Sci. USA* **104**, 15841-15846. doi:10.1073/pnas.0702697104

Low, J. T., Mitchell, J. M., Do, O. H., Bax, J., Rawlings, A., Zavortink, M., Maorgan, G., Parton, R. G., Gaisano, H. Y. and Thorn, P. (2013). Glucose principally regulates insulin secretion in mouse islets by controlling the numbers of granule fusion events per cell. *Diabetologia* **56**, 2629-2637. doi:10.1007/s00125-013-3019-5

Ma, L., Bindokas, V. P., Kuznetsov, A., Rhodes, C., Hays, L., Edwardson, J. M., Ueda, K., Steiner, D. F. and Philipson, L. H. (2004). Direct imaging shows that insulin granule exocytosis occurs by complete vesicle fusion. *Proc. Natl. Acad. Sci. USA* **101**, 9266-9271. doi:10.1073/pnas.0403201101

Miklavc, P., Hecht, E., Hobi, N., Wittekindt, O. H., Dietl, P., Kranz, C. and Frick, M. (2012). Actin coating and compression of fused secretory vesicles are essential for surfactant secretion - a role for Rho, formins and myosin II. *J. Cell Sci.* **125**, 2765-2774. doi:10.1242/jcs.105262

Mourad, N. I., Nenquin, M. and Henquin, J.-C. (2010). Metabolic amplifying pathway increases both phases of insulin secretion independently of β-cell actin microfilaments. *Am. J. Physiol. Cell Physiol.* **299**, C389-C398. doi:10.1152/ajpcell.00138.2010

Muallem, S., Kwiatkowska, K., Xu, X. and Yin, H. L. (1995). Actin filament disassembly is a sufficient final trigger for exocytosis in nonexcitable cells. *J. Cell Biol.* **128**, 589-598. doi:10.1083/jcb.128.4.589

Ñeco, P., Fernández-Peruchena, C., Navas, S., Gutiérrez, L. M., de Toledo, G. A. and Alés, E. (2008). Myosin II contributes to fusion pore expansion during exocytosis. *J. Biol. Chem.* **283**, 10949-10957. doi:10.1074/jbc.M709058200

Nemoto, T., Kojima, T., Oshima, A., Bito, H. and Kasai, H. (2004). Stabilization of exocytosis by dynamic F-actin coating of zymogen granules in pancreatic acini. *J. Biol. Chem.* **279**, 37544-37550. doi:10.1074/jbc.M403976200

Nightingale, T. D., White, I. J., Doyle, E. L., Turmaine, M., Harrison-Lavoie, K. J., Webb, K. F., Cramer, L. P. and Cutler, D. F. (2011). Actomyosin II contractility expels von Willebrand factor from Weibel-Palade bodies during exocytosis. *J. Cell Biol.* **194**, 613-629. doi:10.1083/jcb.201011119

Orci, L., Gabbay, K. H. and Malaisse, W. J. (1972). Pancreatic beta-cell web - its possible role in insulin secretion. *Science* **175**, 1128. doi:10.1126/science.175.4026.1128

Riedl, J., Crevenna, A. H., Kessenbrock, K., Yu, J. H., Neukirchen, D., Bista, M., Bradke, F., Jenne, D., Holak, T. A., Werb, Z. et al. (2008). Lifeact: a versatile marker to visualize F-actin. *Nat. Methods* **5**, 605-607. doi:10.1038/nmeth.1220

Rizvi, S. A., Neidt, E. M., Cui, J., Feiger, Z., Skau, C. T., Gardel, M. L., Kozmin, S. A. and Kovar, D. R. (2009). Identification and characterization of a small molecule inhibitor of formin-mediated actin assembly. *Chem. Biol.* **16**, 1158-1168. doi:10.1016/j.chembiol.2009.10.006

Rousso, T., Schejter, E. D. and Shilo, B.-Z. (2016). Orchestrated content release from Drosophila glue-protein vesicles by a contractile actomyosin network. *Nat. Cell Biol.* **18**, 181-190. doi:10.1038/ncb3288

Shin, W., Ge, L., Arpino, G., Villarreal, S. A., Hamid, E., Liu, H., Zhao, W.-D., Wen, P. J., Chiang, H.-C. and Wu, L.-G. (2018). Visualization of membrane pore in live cells reveals a dynamic-pore theory governing fusion and endocytosis. *Cell* **173**, 934-945.e12. doi:10.1016/j.cell.2018.02.062

Sokac, A. M. and Bement, W. M. (2006). Kiss-and-coat and compartment mixing: coupling exocytosis to signal generation and local actin assembly. *Mol. Biol. Cell* **17**, 1495-1502. doi:10.1091/mbc.e05-10-0908

Sokac, A. M., Co, C., Taunton, J. and Bement, W. (2003). Cdc42-dependent actin polymerization during compensatory endocytosis in Xenopus eggs. *Nat. Cell Biol.* **5**, 727-732. doi:10.1038/ncb1025

Somlyo, A. P. and Somlyo, A. V. (2003). Ca^{2+} sensitivity of smooth muscle and nonmuscle myosin II: modulated by G proteins, kinases, and myosin phosphatase. *Physiol. Rev.* **83**, 1325-1358. doi:10.1152/physrev.00023.2003

Suarez, C. and Kovar, D. R. (2016). Internetwork competition for monomers governs actin cytoskeleton organization. *Nat. Rev. Mol. Cell Biol.* **17**, 799-810. doi:10.1038/nrm.2016.106

Sun, Y., Leong, N. T., Wong, T. and Drubin, D. G. (2015). A Pan1/End3/Sla1 complex links Arp2/3-mediated actin assembly to sites of clathrin-mediated endocytosis. *Mol. Biol. Cell* **26**, 3841-3856. doi:10.1091/mbc.E15-04-0252

Takahashi, N., Kishimoto, T., Nemoto, T., Kadowaki, T. and Kasai, H. (2002). Fusion pore dynamics and insulin granule exocytosis in the pancreatic islet. *Science* **297**, 1349-1352. doi:10.1126/science.1073806

Tomas, A., Yermen, B., Min, L., Pessin, J. E. and Halban, P. A. (2006). Regulation of pancreatic beta-cell insulin secretion by actin cytoskeleton remodelling: role of gelsolin and cooperation with the MAPK signalling pathway. *J. Cell Sci.* **119**, 2156-2167. doi:10.1242/jcs.02942

Tran, D. T., Masedunskas, A., Weigert, R. and Ten Hagen, K. G. (2015). Arp2/3-mediated F-actin formation controls regulated exocytosis in vivo. *Nat. Commun.* **6**, 10098. doi:10.1038/ncomms10098

Tsuboi, T., Mcmahon, H. T. and Rutter, G. A. (2004). Mechanisms of dense core vesicle recapture following "kiss and run" ("cavicapture") exocytosis in insulin-secreting cells. *J. Biol. Chem.* **279**, 47115-47124. doi:10.1074/jbc.M408179200

Turvey, M. R. and Thorn, P. (2004). Lysine-fixable dye tracing of exocytosis shows F-actin coating is a step that follows granule fusion in pancreatic acinar cells. *Pflugers Arch.* **448**, 552-555. doi:10.1007/s00424-004-1288-z

Uenishi, E., Shibasaki, T., Takahashi, H., Seki, C., Hamaguchi, H., Yasuda, T., Tatebe, M., Oiso, Y., Takenawa, T. and Seino, S. (2013). Actin dynamics

regulated by the balance of neuronal Wiskott-Aldrich Syndrome Protein (N-WASP) and cofilin activities determines the biphasic response of glucose-induced insulin secretion. *J. Biol. Chem.* **288**, 25851-25864. doi:10.1074/jbc.M113.464420

Valentijn, K. M., Gumkowski, F. D. and Jamieson, J. D. (1999). The subapical actin cytoskeleton regulates secretion and membrane retrieval in pancreatic acinar cells. *J. Cell Sci.* **112**, 81-96.

Valentijn, J. A., Valentijn, K., Pastore, L. M. and Jamieson, J. D. (2000). Actin coating of secretory granules during regulated exocytosis correlates with the release of rab3D. *Proc. Natl. Acad. Sci. USA* **97**, 1091-1095. doi:10.1073/pnas.97.3.1091

Wang, Z. X., Oh, E. J. and Thurmond, D. C. (2007). Glucose-stimulated Cdc42 signaling is essential for the second phase of insulin secretion. *J. Biol. Chem.* **282**, 9536-9546. doi:10.1074/jbc.M610553200

Wen, P. J., Grenklo, S., Arpino, G., Tan, X., Liao, H.-S., Heureaux, J., Peng, S.-Y., Chiang, H.-C., Hamid, E., Zhao, W.-D. et al. (2016). Actin dynamics provides membrane tension to merge fusing vesicles into the plasma membrane. *Nat. Commun.* **7**, 12604. doi:10.1038/ncomms12604

Wu, C., Asokan, S. B., Berginski, M. E., Haynes, E. M., Sharpless, N. E., Griffith, J. D., Gomez, S. M. and Bear, J. E. (2012). Arp2/3 is critical for lamellipodia and response to extracellular matrix cues but is dispensable for chemotaxis. *Cell* **148**, 973-987. doi:10.1016/j.cell.2011.12.034

Yang, Q., Zhang, X.-F., Pollard, T. D. and Forscher, P. (2012). Arp2/3 complex-dependent actin networks constrain myosin II function in driving retrograde actin flow. *J. Cell Biol.* **197**, 939-956. doi:10.1083/jcb.201111052

Yu, H.-Y. E. and Bement, W. M. (2007). Control of local actin assembly by membrane fusion-dependent compartment mixing. *Nat. Cell Biol.* **9**, 149-159. doi:10.1038/ncb1527

Yuan, T., Liu, L., Zhang, Y., Wei, L., Zhao, S., Zheng, X., Huang, X., Boulanger, J., Gueudry, C., Lu, J. et al. (2015). Diacylglycerol guides the hopping of clathrin-coated pits along microtubules for exo-endocytosis coupling. *Dev. Cell* **35**, 120-130. doi:10.1016/j.devcel.2015.09.004